



# THE UPPER ATMOSPHERE OVER PERU

FEBRUARY 2024



This report provides observations recorded in February 2024, during the current solar cycle 25, which is approaching the solar maximum. Several X-class solar flares were detected, including the most intense solar flare (X6.3) in the current solar cycle, as presented in Figure 1. Our measurements observed the flare’s impacts on the ionosphere, including the magnetic field at the magnetic equator (magnetic crochet in Figure 5) and D-layer absorption in the ionogram as depicted in Figure 6.

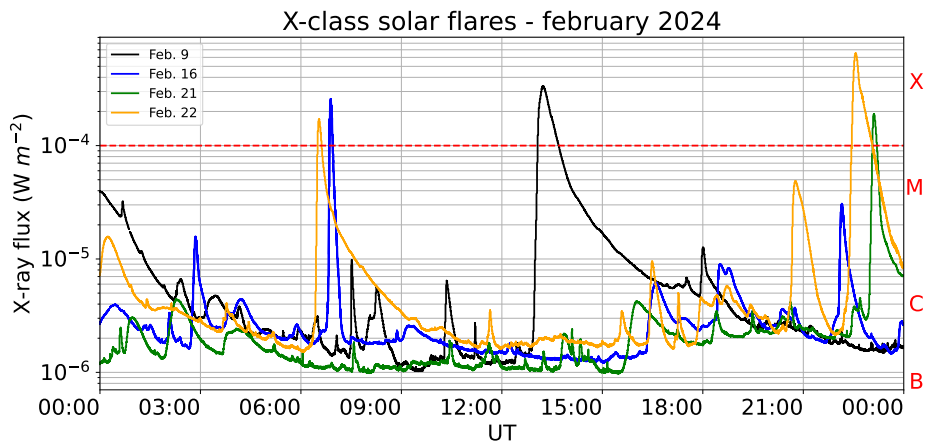


Figure 1. X-class solar flares occurred during February 2024. Data obtained from the GOES-16 satellite mission database[1].

Table 1. Summary of monthly measurements of some ionospheric parameters and space weather predominant conditions. February 2024.

Average MLT winds a 90 km [m/s]		Maximum diurnal variation of the horizontal component of the geomagnetic field (H)[nT]		Average vertical plasma drifts (300 km- 400 km) [m/s]	
Meridional	Zonal	LIM:132	AQP:81	Min.	Max.
Min: 35.8 S	Min: 18.7 O	HYO: 121	NZC: 85	-33	40
Max: 38.6 N	Máx: 6.4 E	PIU: 80			
GEOMAGNETIC ACTIVITY: QUIET			SOLAR ACTIVITY: HIGH		

## DID YOU KNOW THAT?

We are approaching the maximum of the current solar cycle (25) (predicted to be in July 2025[2]), which brings an enhancement of the solar radiation incidence into the ionosphere and, hence, a higher electron density, as shown in the ionogram (Figure 4[3]). On the other hand, the increase of solar activity leads to a higher occurrence of X-class solar flares, the most intense of all. This behavior is exhibited in Figure 2, where the monthly number of X-class solar flares for solar cycles 23 and 24 is shown. Although solar flares emit throughout the whole electromagnetic spectrum, the strengthening of X-ray ( $\lambda < 10$  nm) and UV ( $\lambda < 200$  nm) emissions (the former in a factor of ten and the latter, in 10% ) is the signature that distinguishes them. Accordingly, solar flare classification is based on the GOES XRS X-ray sensor measurements mounted inside GOES[3] between 0.1 nm and 0.8 nm, consisting of a letter and a number. This way, the letter indicated a negative power of 10 for the irradiance peak: A ( $10^{-8}$  W/m<sup>2</sup>), B ( $10^{-7}$  W/m<sup>2</sup>), C ( $10^{-6}$  W/m<sup>2</sup>), M ( $10^{-5}$  W/m<sup>2</sup>), X ( $10^{-4}$  W/m<sup>2</sup>) and the number (less

than 10) is the coefficient that multiplies the negative power of 10 already mentioned[4]. For instance, a class X1.7 solar flare means that its emission peak within 0.1 nm and 0.8 nm was  $1.7 \times 10^{-4}$  W/m<sup>2</sup>.

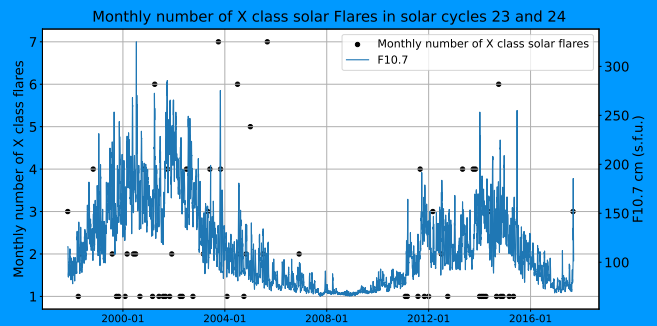


Figure 2. Monthly number of X-class solar flares during solar cycles 23 and 24. Data obtained from "Characteristics of X-class flares of solar cycles 23 and 24 in X-ray and EUV bands". Adv. Space Res., 71(12) (2023)[4].

## 1. Climatology

The geomagnetic activity (Kp[5] index) was generally quiet 98% of the time, 1% moderate, and 1% strong; however, the solar activity (F10.7[6] index) was high 86% of the time, and moderate 14% (Figure 3 and Table 1). Previous studies have shown that there is a significant relationship between the daily and seasonal variation of the horizontal component of the geomagnetic field (H)[7], which is reflected in our observations.

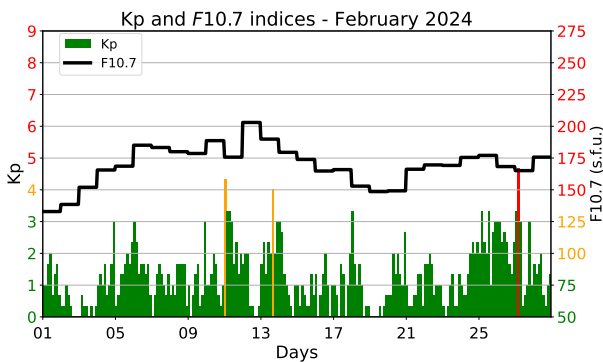


Figure 3. Kp y F10.7 cm (u.f.s. =  $10^{-22}$ Wm<sup>-2</sup>Hz<sup>-1</sup>) values for february. Retrieved from OMNIWeb[8].

In the months close to the March equinox and with high or moderate solar activity, Spread-F is expected to occur more frequently in the hours before midnight,

between 250 and 600 km. On the other hand, few events are expected to occur after midnight, previous measurements show excellent agreement with climatology[9]. Furthermore, the February climatology for low or moderate solar activity (given by the Scherliess-Fejer model) indicates that the height average (300-400 km) of vertical plasma drifts is approximately -20 m/s after midnight, increasing to 15 m/s at 10:30 LT. Following that, these values decrease up to 7 m/s at 17:00 LT, when they begin to increase due to the pre-reversal enhancement[10] phenomena, up to 25 m/s at 19:30 LT, and then decrease to -20 m/s before midnight.

The values of the climatology show moderate agreement with the measurements except for hours around the pre-reversal enhancement.

Climatological studies[11] point out that for months near the March equinox, the 150 km echoes appear around 9:00 LT, disappear after 15:30 LT, and are detected between 140 and 165 km. Measurements show great agreement with climatology.

## 2. Increase on solar activity

As we approach the maximum of the current solar cycle, a steady increase in solar activity is manifested in

several ways, including increased ionospheric electron density and a higher frequency of X-class solar flares. For the low solar activity period, previously recorded ionogram traces show a typical frequency range between 3 MHz and 12 MHz at 10 AM, but as the solar activity increased the ionospheric density and plasma frequency also increased as a result plasma frequency matched with the transmitted signal by the ionosonde to achieve signal reflection (Figure 4). On 22 February, the solar flare caused extra ionization in the ionosphere, which sustained the presence of additional currents, increasing the values of H-component measurements on magnetometers closer to the magnetic equator (Jicamarca, Huancayo, and Nazca), resulting in the appearance of a magnetic crochet[12], as shown in Figure 5. Additionally, this flare also caused the absorption of part of the signals emitted by the ionosonde at the D-layer[13], as shown in Figure 6.

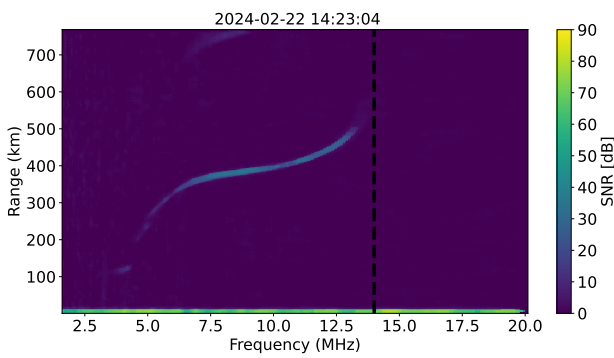


Figure 4. Ionogram illustrating the enhancement of plasma frequency, passing 14 MHz, for the signals received back by the ionosonde in comparison to those at low solar activity regime as a consequence of the increase of electron density due to a higher solar activity[14].

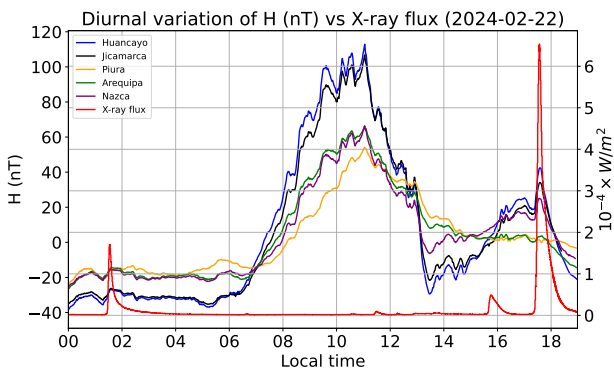


Figure 5. Magnetic crochet caused by a X6.3 class solar flare occurred on February 22 (starting around 17:08 local time). The effect is more noticeable for stations closer to the magnetic equator.

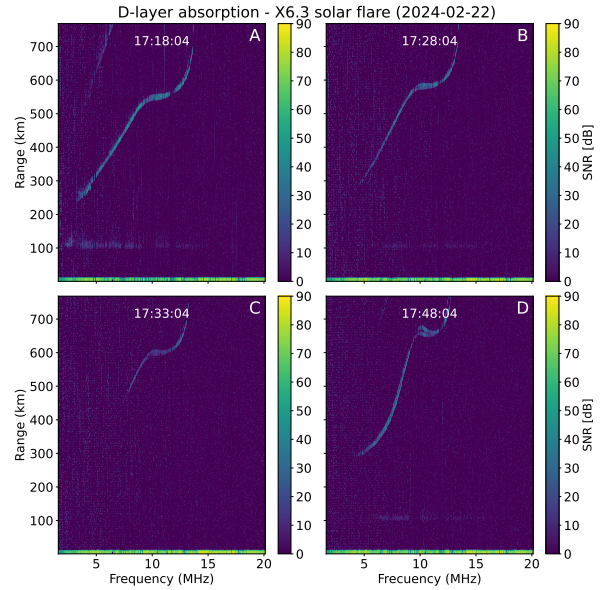


Figure 6. Temporary disappearance of the echoes detected by the ionosonde due to D-layer absorption caused by the X6.3 class solar flare on February 22, the most intense in the current solar cycle so far, can be seen starting at panel B.

### 3. Radar observations on the peruvian upper atmosphere

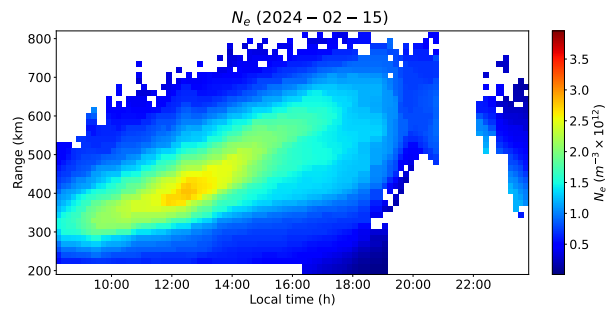


Figure 7. ISR average vertical drifts for February. The red curve represents the height average between 300 and 400 km and the black curve, the predicted values by the Scherliess-Fejer model.

Vertical plasma drift estimated between 300 and 400 km with the Jicamarca Radio Observatory's main radar, a facility of the Instituto Geofísico del Perú (IGP-ROJ) with the JULIA-MP mode and during the campaign to support satellites (February 15th-19th), as shown in Figure 7. These measurements show that the vertical drift average started around -30 m/s (downward) after midnight, then they started to decrease until -33 m/s at 04:30 LT. After that, the drifts increased until they changed their direction (upward) minutes before 08:00 LT. Then, their value increased to 10 m/s at 11:30 LT. Thereafter, vertical drift decreased until the sudden increase at 19:30 LT

known as pre-reversal enhancement[10], with values close to 40 m/s. The estimations after 19:30 LT were contaminated due to the presence of Spread-F echoes. The predicted values from the Scherliess-Fejer model exhibit moderate agreement with the measurements, where the biggest difference was 14 m/s at 21:30 LT.

Additionally, the satellite support campaign included estimations of electron densities at F-region, where the maximum value was  $3.2 \times 10^{12}$  on February 15th at 12:25 LT, as shown in Figure 8.

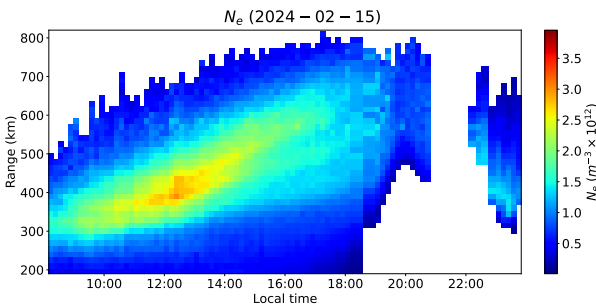


Figure 8. Electron density corresponding to February 15th.

On the other hand, 14 days of measurements for the 150-km Echoes drifts were performed, to further investigate the transition region between E and F-layers. We can notice in Figure 9 that echoes start from 08:00 LT to around 15:30 LT and are contained from 130 km and 165 km high, which agrees with the climatology.

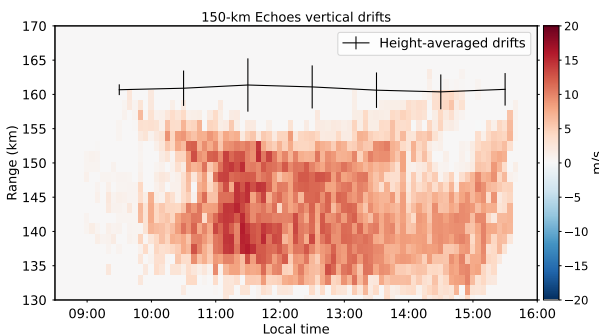


Figure 9. 150-km echoes monthly average vertical drifts. The black curve corresponds to the height-averaged drifts.

In addition, 10 nights of measurements were carried out with the AMISR-14[15] radar system, a period during which the incidence of 10 F-layer irregularities were found in 10 nights, contained between the 200 km and 800 km altitude. The dominant morphology was the Radar Plume type, with 80% occurrence, seconded by the Bottom-type and Post-midnight types, with 10% each, as seen in Figure 10. These observations agree with what is expected from the climatology (performed with the

main radar JULIA mode)[9].

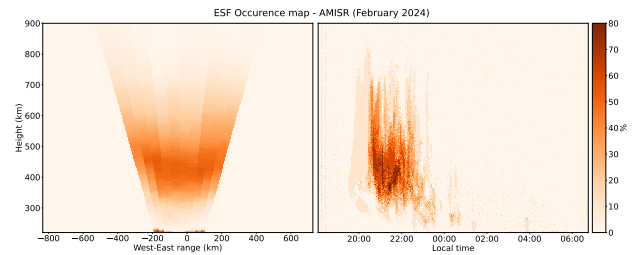


Figure 10. Right panel: traditional occurrence map. Left panel: polar occurrence map.

The time and height average zonal and meridional winds for February 2024 (as shown in Figure 11), exhibit predominant periods of 12-hour and 24-hours (semidiurnal and diurnal solar tides, respectively). In the mesopause ( $\sim 90$  km) it is observed that the value of the maximum average zonal wind was +6.4 m/s at 05:00 hours and the minimum average value was -18.7 m/s at 01:00 hours, while the maximum average of meridional wind was +38.6 m/s at 18:30 hours and the minimum average was -35.8 m/s at 01:30 hours. The maximum zonal wind was +83.9 m/s at 8:15 hours on February 8 and the minimum -97.2 m/s at 8:45 hours on February 18, while the maximum meridional wind was 93.9 m/s at 16:15 hours on February 3rd and the minimum -93.2 m/s at 12:45 hours on February 7th.

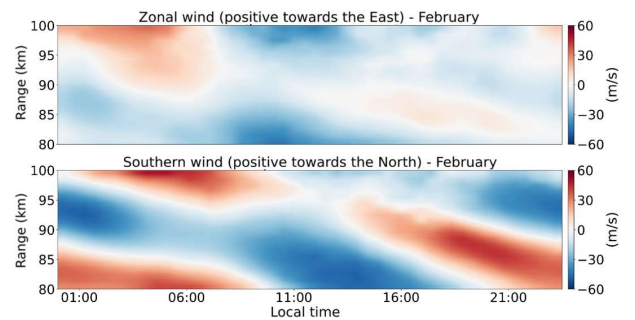


Figure 11. Monthly average zonal and meridional winds for the month of February 2024.

## 4. LISN Observations

Measurements of the horizontal component H of the geomagnetic field at the IGP-JRO magnetic stations is presented in Figure 12. The average values of the Jicamarca and Huancayo stations were higher than those of the other sites because they are located on the geomagnetic equator, and the Equatorial Electrojet

(EEJ) adds to an increase in their measurements. Furthermore, there was significant daily variability, particularly around 11:00 hours (16:00 hours UTC). The maximum and minimum variations of the monthly average values for February were recorded for each station: Piura (81 nT), Huancayo (131 nT), Jicamarca (132 nT), Arequipa (81 nT), and Nazca (85 nT).

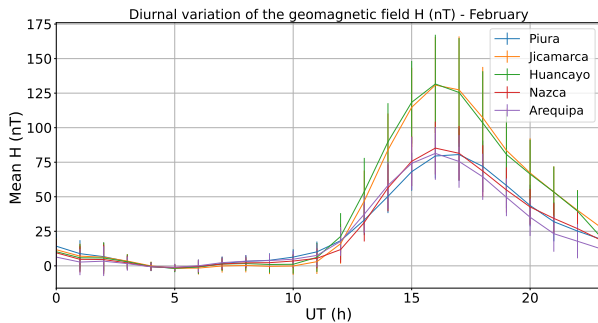


Figure 12. Hourly monthly average values of the diurnal variation of H-component for all of our magnetic stations operating during February 2024.

Amplitude scintillation index (S4) data for the Jaén, IGP-JRO, Pontifical Catholic University of Peru, and Cuzco stations is shown in Figure 13. Low, moderate, and high scintillation activity levels were recorded during the investigation. The highest S4 index value was 1.4, recorded at the Cuzco Station around 00:27 (local time) on February 25th.

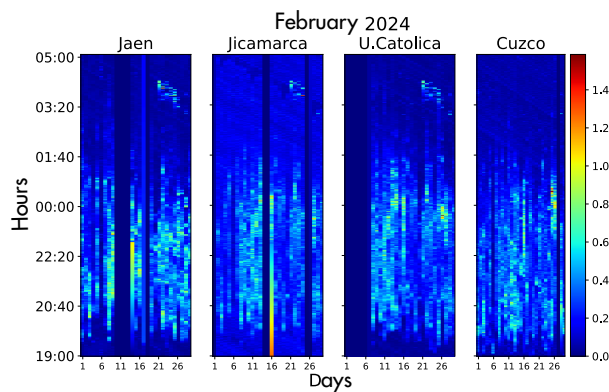


Figure 13. S4 maximum daily values for the Jaén, Jicamarca, Catholic University of Perú and Cuzco stations during February 2024. Low, moderate and high scintillation activity regimes were observed.

## 5. Conclusions

- A high occurrence of X-class solar flares was registered as a consequence of the proximity to the current solar cycle maximum.

- A magnetic crochet and D-layer absorption were observed as effects of the most intense solar flare in the current solar cycle so far.
- Low, moderate, and high scintillation activities were reported, with 1.4 highest S4 index value (Cuzco station at 00:27 on February 25).

## 6. Referencias

- [1] "Index of /platforms/solar-space-observing-satellites/goes/goes16/11b/docs," Mar 2024, Accessed on: Mar. 19, 2024. [Online]. Available: <https://data.ngdc.noaa.gov/platforms/solar-space-observing-satellites/goes/goes16/11b/docs/>
- [2] N. W. Service, "Hello Solar Cycle 25. NOAA's National Weather Service." 2020. [Online]. Available: <https://www.weather.gov/news/201509-solar-cycle>
- [3] D. J. Gorney, "Solar cycle effects on the near-earth space environment," vol. 28(3), p. 315–336, 1990. [Online]. Available: [doi:10.1029/RG028i003p00315](https://doi.org/10.1029/RG028i003p00315)
- [4] K. Pandey, D. Chakrabarty, A. Kumar, A. Bhardwaj, S. Biswal, G. C. Hussey, and A. K. Yadav, "Characteristics of x-class flares of solar cycles 23 and 24 in x-ray and ev bands." vol. 71(12), p. 5438–5452, 2023. [Online]. Available: [doi:10.1016/j.asr.2023.02.022](https://doi.org/10.1016/j.asr.2023.02.022)
- [5] "The Kp-index | Help," Oct 2020, Accessed on: Feb. 01, 2023. [Online]. Available: <https://www.spaceweatherlive.com/en/help/the-kp-index.html>
- [6] "F10.7 cm Radio Emissions | NOAA / NWS Space Weather Prediction Center," Jul 2020, Accessed on: Feb. 01, 2023. [Online]. Available: <https://www.swpc.noaa.gov/phenomena/f107-cm-radio-emissions>
- [7] I. Adimula, K. Gidado, and S. Bello, "Variability of horizontal magnetic field intensity from some stations within the equatorial electrojet belt," *Physical Science International Journal*, vol. 13, pp. 1–8, 01 2017.
- [8] N. Papitashvili, "OMNIWeb Data Explorer," Oct 2020, Accessed on: Mar. 16, 2023. [Online]. Available: <https://omniweb.gsfc.nasa.gov/form/dx1.html>
- [9] W. Zhan, F. S. Rodrigues, and M. A. Milla, "On the genesis of postmidnight equatorial spread f: Results for the american/peruvian sector," *Geophysical Research Letters*, vol. 45, no. 15, pp. 7354–7361, 2018.

- [10] J. V. Eccles, J. P. St. Maurice, and R. W. Schunk, "Mechanisms underlying the pre-reversal enhancement of the vertical plasma drift in the low-latitude ionosphere." *J. Geophys. Res. Space Physics*, vol. 120, p. 4950–4970, 2015.
- [11] J. L. Chau and E. Kudeki, "Statistics of 150-km echoes over jicamarca based on low-power vhf observations," *Ann. Geophys.*, p. 1305–1310, 2006.
- [12] J. J. Curto, "Geomagnetic solar flare effects: a review. *J. Space Weather Space Clim*," 2020. [Online]. Available: [doi:10.1051/swsc/20200271](https://doi.org/10.1051/swsc/20200271)
- [13] I. G. del Perú, "Realtime at jicamarca," Mar. 2022, [Online; accessed 21. Mar. 2024]. [Online]. Available: [https://www.igp.gob.pe/observatorios/radio-observatorio-jicamarca/realtime/static/reports/2022/Boletin\\_Marzo\\_2022.pdf](https://www.igp.gob.pe/observatorios/radio-observatorio-jicamarca/realtime/static/reports/2022/Boletin_Marzo_2022.pdf)
- [14] H. Vickers, M. J. Kosch, E. S. an L. Bjoland, Y. Ogawa, and C. L. Hoz, "A solar cycle of upper thermosphere density observations from the EISCAT Svalbard Radar," *J. Geophys. Res. Space Physics*, vol. 119, p. 6833–6845, 2014.
- [15] " Instituto Geofísico del Perú, "Realtime at Jicamarca" ," Aug. 2022, [Online; accessed 29. Aug. 2022]. [Online]. Available: <https://www.igp.gob.pe/observatorios/radio-observatorio-jicamarca/realtime/tools>

**Developed by:**

BA. Juan Pablo Velásquez Ormaeche  
 BA. Roberto Flores Arroyo  
 MA. Luis Condori Illahuamán  
 PhD. Edgardo Pacheco Josan

**Design and layout:**

BA. Anette De la Cruz Meza

**Collaborators:**

MA. Karim Kuyeng Ruiz  
 PhD. Danny Scipión Castillo  
 PhD. Marco Milla Bravo

**Contact:**

[roj@igp.gob.pe](mailto:roj@igp.gob.pe)